

# **The Inelastic Mean Free Path (IMFP): Theory, Experiment, and Applications**

**S. Tanuma, C. J. Powell\*, D. R. Penn\*, and K. Goto\*\***

National Institute for Materials Science (NIMS)

\*National Institute of Standards and Technology (NIST)

\*\*National Institute of Advanced Industrial Science and Technology Chubu

- 1. Introduction**
- 2. Calculation of IMFPs from optical data**
  - Evaluation of energy-loss function data
  - Fano Plots - Modified Bethe equation fits
  - Comparison with IMFPs from the TPP-2M equation
- 3. Experimental determination of IMFPs**
  - Results for 13 elemental solids
- 4. IMFP Applications**
  - Effective attenuation lengths
  - Mean escape depths
  - Information depths
  - Modeling XPS for Thin-Film Structures
- 5. Summary**

1

I will be talking about Electron scattering in Surface electron spectroscopy. My talk consists of 4 part.

The first is introduction.

The second is calculations of IMFPs for wide variety of materials. I will talk about the evaluation of energy loss functions, Fano Plot,.....

The third is experimental determinations of IMFPs with elastic peak electron spectroscopy. The last is summary.

# 1. Introduction

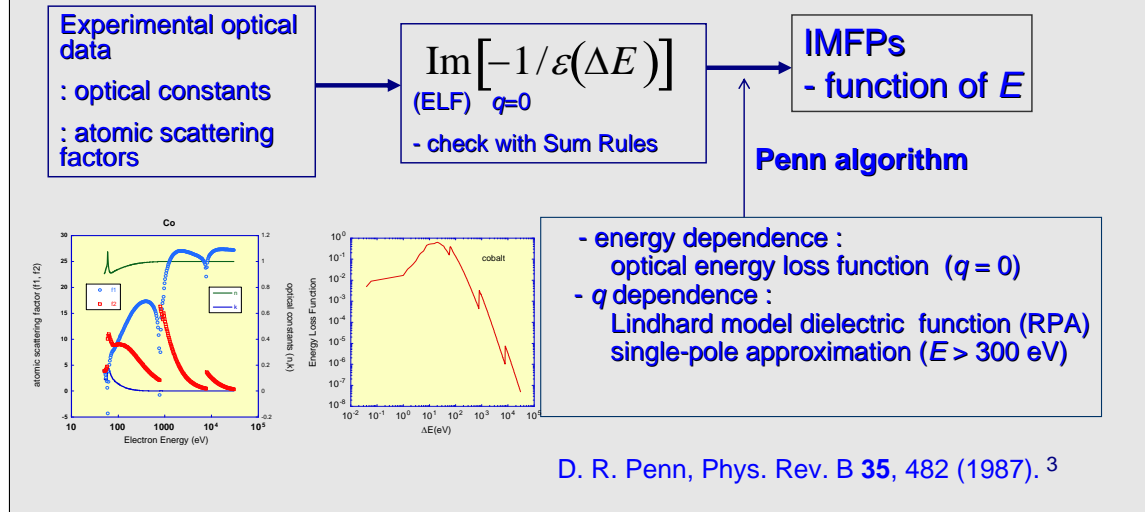
- The electron inelastic mean free path (IMFP) is a basic material parameter for describing the surface sensitivity of XPS and other surface electron spectroscopies.
- IMFP is needed for quantitative analyses by XPS (“matrix correction”), determination of film thicknesses (with effective attenuation lengths), and estimates of surface sensitivity (mean escape depths and information depths).
- IMFPs have been determined for 75 materials from optical energy-loss functions with the Penn algorithm for energies from 50 eV to 30,000 eV (previously 50 eV to 2,000 eV)
- The TPP-2M formula for predicting IMFPs has been evaluated for the 50 eV to 30,000 eV range (previously 50 eV to 2,000 eV)

## 2. Calculation of IMFPs from optical data

- Flow of calculation

$$\frac{d^2\sigma}{dq d\omega} = \frac{me_0^2}{\pi N h E} \operatorname{Im} \left( \frac{-1}{\varepsilon(q, \omega)} \right) \frac{1}{q}$$

$$n\sigma\lambda = 1$$



This shows the flow of IMFP calculation from energy loss function.

Electron inelastic mean free path in solid can be calculated from imaginary part of inverse dielectric function or energy loss function.

In Penn algorithm, the energy dependence of ELF can be obtained from experimental optical energy loss function. As for  $q$ -dependence, it is very difficult to measure with experimental method. Then the Lindhard model dielectric function was used. Over 300 eV, we used the single pole approximation for  $q$ -dependence of ELF.

## Conditions and materials for IMFP calculations

- Energy range for IMFP calculation: 50 eV to 30,000 eV
  - calculated at equal intervals on a logarithmic energy scale corresponding to increases of 10 %.
- 42 elemental solids
  - Li, Be, diamond, graphite, glassy carbon, Na, Mg, Al, Si, K, Sc, Ti, V, Cr, Fe, Co, Ni, Cu, Ge, Y, Zr, Nb, Mo, Ru, Rh, Pd, Ag, In, Sn, Cs, Gd, Tb, Dy, Hf, Ta, W, Re, Os, Ir, Pt, Au, and Bi
- 12 organic compounds
  - 26-n-paraffin, adenine, beta-carotene, diphenyl-hexatriene, guanine, kapton, polyacetylene, poly(butene-1-sulfone), polyethylene, polymethylmethacrylate, polystyrene, and poly(2-vinylpyridine)
- 21 inorganic compounds
  - $\text{Al}_2\text{O}_3$ , GaAs, GaP,  $\text{H}_2\text{O}$ , InAs, InP, InSb, KBr, KCl, LiF, MgO, NaCl,  $\text{NbC}_{0.712}$ ,  $\text{NbC}_{0.844}$ ,  $\text{NbC}_{0.93}$ , PbS, SiC,  $\text{SiO}_2$ ,  $\text{VC}_{0.758}$ ,  $\text{VC}_{0.858}$  and ZnS.

4

The IMFPs were calculated in the 50eV to 30 keV energy range.

They were calculated at equal intervals...

These show the list of the calculated materials.

We have calculated these 42 elemental solids, 12 organic compounds and 21 inorganic compounds as shown here.

Because they have optical constants sufficient energy range.

## Evaluations of Energy-Loss Functions with Sum Rules

f-sum rule (or oscillator-strength sum rule)

$$Z_{eff} = (2 / \pi \hbar^2 \Omega_p^2) \int_0^{\Delta E_{max}} \Delta E \text{Im}[-1 / \varepsilon(\Delta E)] d(\Delta E)$$

KK-sum rule (a limiting form of the Kramers-Kronig integral)

$$P_{eff} = (2 / \pi) \int_0^{\Delta E_{max}} \Delta E^{-1} \text{Im}[-1 / \varepsilon(\Delta E)] d(\Delta E) + n^{-2}(0)$$

When  $\Delta E_{max} \rightarrow \infty$

$$Z_{eff} \rightarrow Z$$

$$P_{eff} \rightarrow 1$$

: total number of electrons  
for material

5

The accuracy of the energy loss function affects the reliability of IMFPs.

Then it is very important to evaluate energy loss function with sum rules.

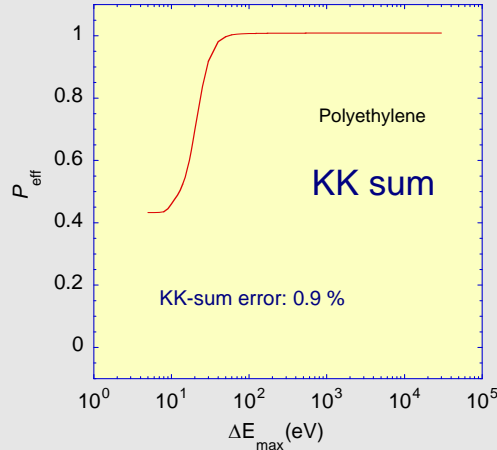
We use two effective sum rules.

Using F-sum rule, we can evaluate the accuracy of ELF at high energy region.

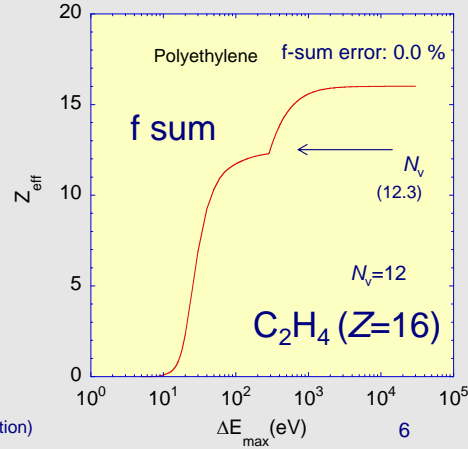
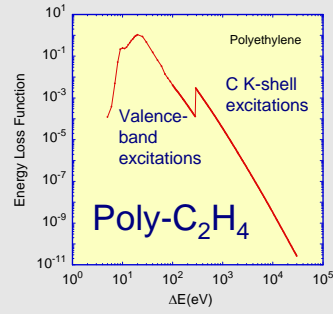
With KK-sum rule, the accuracy of low energy region of ELF, especially under 100 eV, can be evaluated.

When  $\Delta E_{max}$  becomes infinity, f-sum value  $Z_{eff}$  equals to the total number of electron for material and  $P_{eff}$  equals to unity if ELF is correct.

## Energy loss function and sum-rule calculations for organic compounds (e.g., polyethylene)



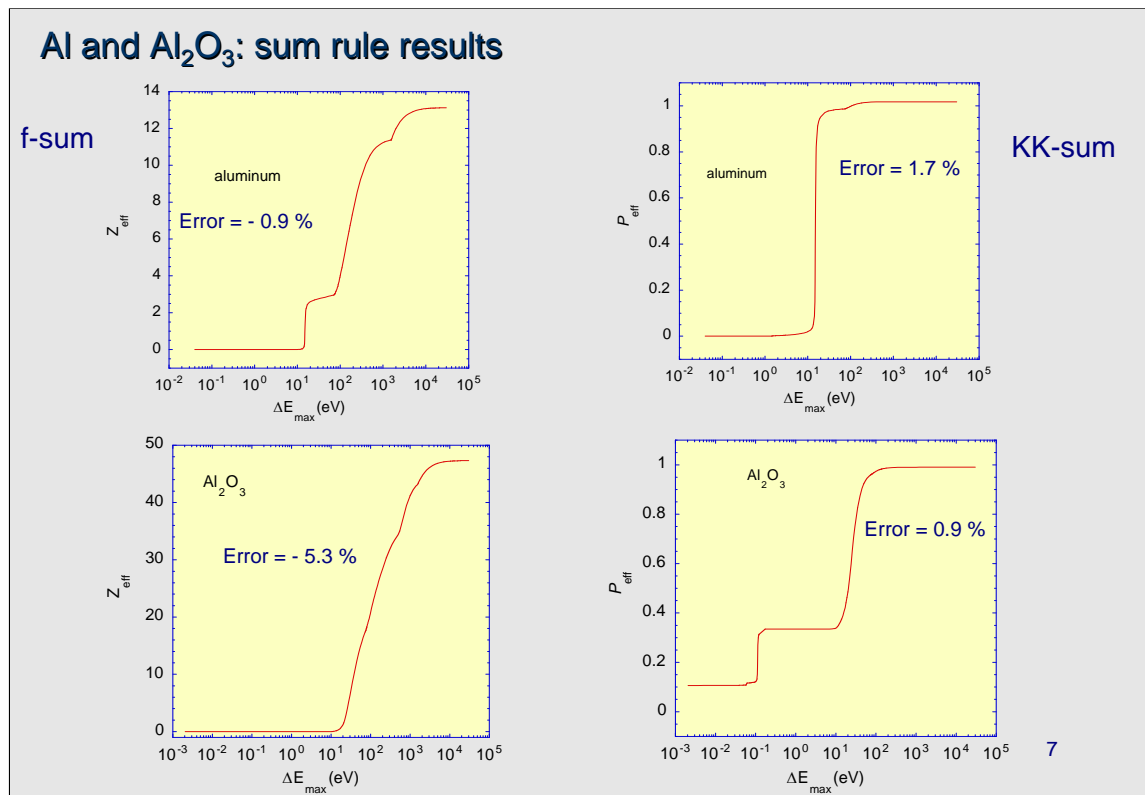
:saturates over 60 eV  
:evaluated low-energy region (and  $n(0)$  value gave large contribution)



This shows the results of sum rule calculations for polyethylene. This is the energy loss function of polyethylene. Since polyethylene consists of low atomic number elements Hydrogen and carbon, its ELF is very simple.

This peak corresponds to the valence and conduction electron excitation. This is due to the carbon K-shell ionization.

This figure shows the F-sum rule results. We see the contribution of valence electrons ;  $N_v = 12.3$  this value is almost the same as theoretical value.

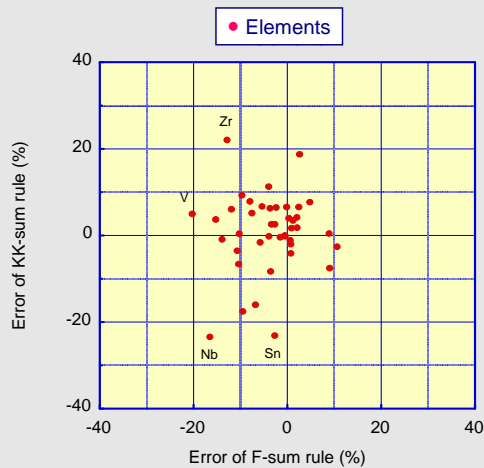


These figures are the calculated results of sum rule for aluminum and aluminum oxide.

Theoretical values Al = 13 (total electrons )  
 Al<sub>2</sub>O<sub>3</sub> =50. The error of f-sum rule for Al is -0.9%, -5.3 % for Al<sub>2</sub>O<sub>3</sub>.

- Valence electrons : 3 for Al not clear Al<sub>2</sub>O<sub>3</sub>
- K-shell :about 2 for Al:
- For Al<sub>2</sub>O<sub>3</sub> : the shell structure is not clear compared to Al

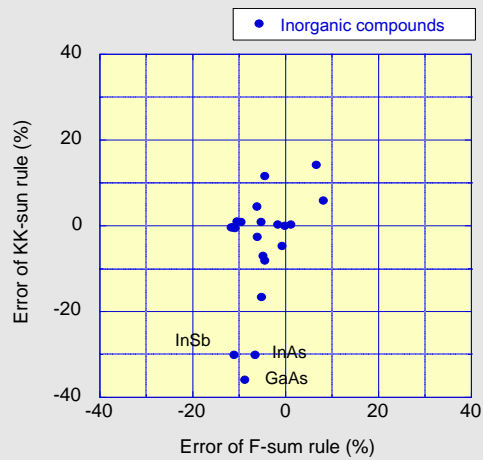
## Sum-rule results for elemental solids and inorganic compounds



Results for 42 elemental solids

RMS KK-sum error: 9.0 %

RMS f-sum error: 7.6 %



Results for 21 inorganic compounds

RMS KK-sum error: 14% (6.7%)

RMS f-sum error: 7.4 %

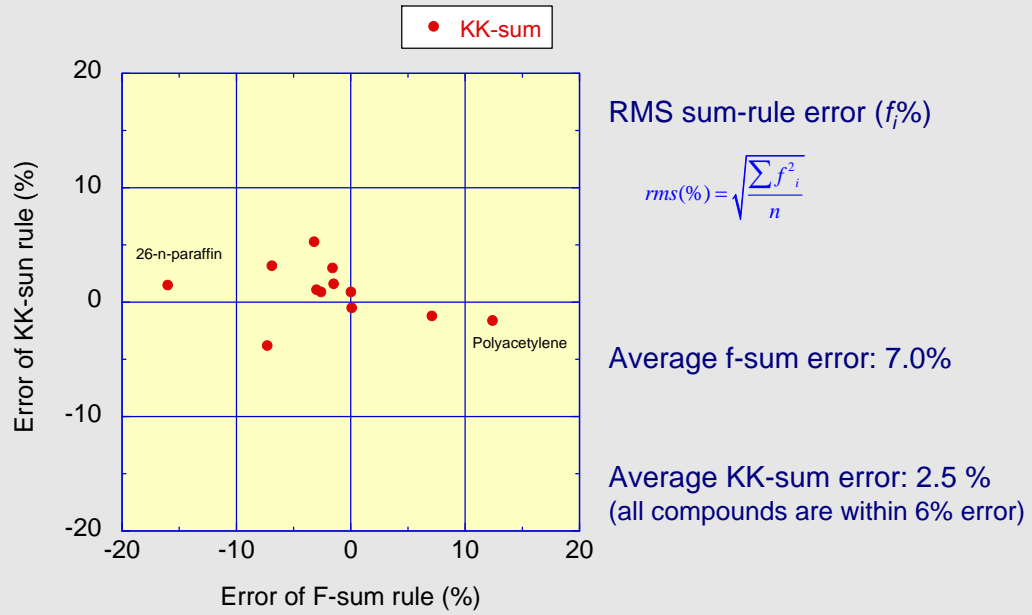
8

These figures show the results of sum rule calculations for elements and inorganic compounds. For 42 elemental solids, the root mean square error of KK-sum rules is 9.0 %. F-sum rule error is 7.8% . These values indicate these ELF are sufficiently accurate for IMFP calculations.

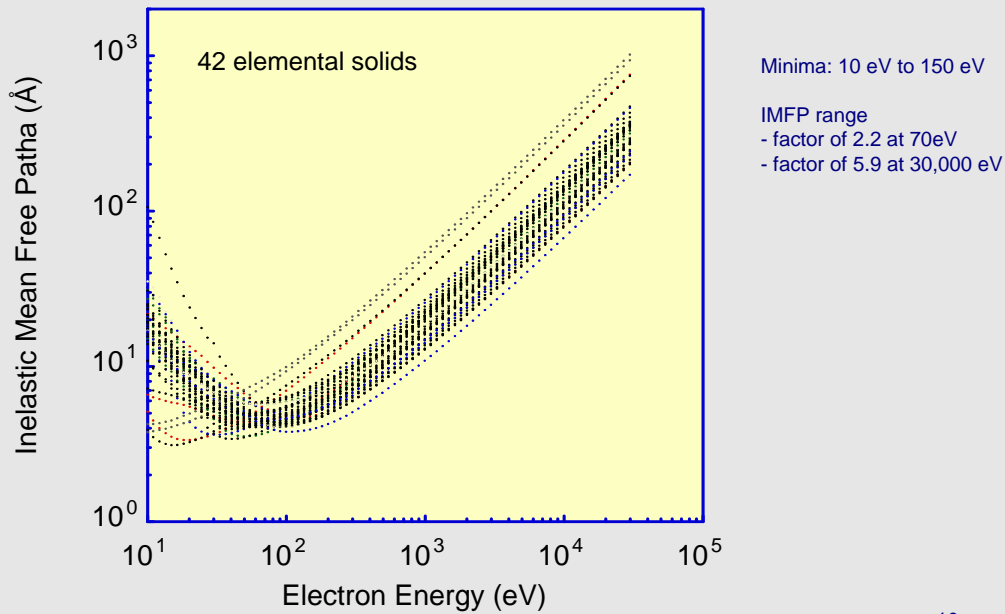
As for these compounds and elements, we plan to measure optical constants by EELS.

We also plan to calculate optical constants from band structure calculations. yesterday my colleague Shinotuka talked about the calculation of optical constants for several metals.

## Sum-rule results for organic compounds



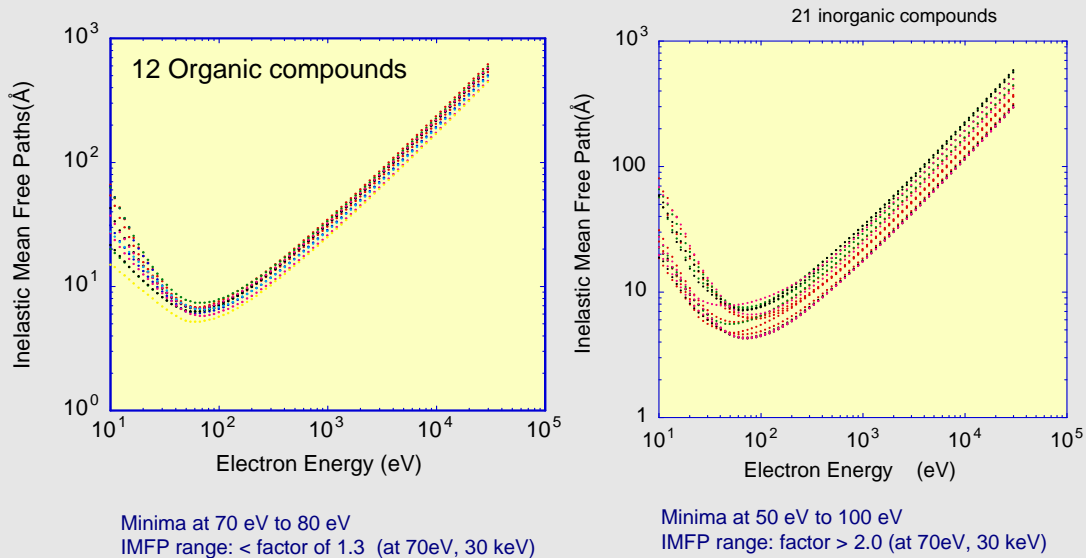
## Calculated IMFPs for 42 elemental solids



This shows the calculated IMFPs for 42 elemental solids as functions of electron energy in the 10 eV to 30 000 eV energy range. We see the minimum values are in the vicinity of 70 eV.

There are large variation at 30 000 eV and very low energy region. The factor at 30 000 eV is 5.9. This means very large material dependence.

## Calculated IMFPs for compounds



11

These figures show the calculated IMFPs as functions of electron energy for 12 organic compounds and 21 elemental solids.

For organic compounds, there are minimum values around 70 - 80 eV. The factor is small, 1.3 at 70 eV and 30 000 eV.

This is the reason why their variation of valence electron density are small for organic compounds.

In 21 organic compounds, the minimum points are in the 50 to 100 eV energy range. In the 70 to 30 000, the material dependence is almost constant. It is about 2.0.

## Modified Bethe equation for IMFP

Bethe equation for total inelastic-scattering cross section in matter at electron energy  $E$

$$\sigma_{\text{tot}} = \frac{4\pi a_0^2}{(E/R)} M_{\text{tot}}^2 \ln\left(\frac{4c_{\text{tot}} E}{R}\right)$$

$$M_{\text{tot}}^2 = \int_0^{\Delta E_{\text{max}}} \frac{2R \operatorname{Im}[-1/\epsilon(\Delta E)] d(\Delta E)}{\pi \hbar^2 \Omega_p^2}$$



IMFP equation: Modified Bethe equation for 50 eV to 30,000 eV range

$$\lambda = \frac{E}{E_p^2 [\beta \ln(\gamma E) - C/E + D/E^2]}$$

$E_p$  = bulk plasmon energy  
 $\beta, \gamma, C,$  and  $D$  are parameters

M. Inokuti, Rev. Mod. Phys. **43**, 297 (1971).

12

The Bethe..... can be described as this equation.  
 $M_{\text{tot}}^2$  square of dipole matrix elements for all possible scattering process.  
 Based on this equation, we derived this equation for describing IMFPs in the 50 – 30,000 eV, We call it modified Bethe equation for IMFP.

Analysis of energy dependence of IMFPs by Fano Plots:  
50 eV to 30 000 eV

$$\lambda = \frac{E}{E_p^2 [\beta \ln(\gamma E) - C/E + D/E^2]} \quad (\text{\AA})$$

Fano plot:  
 $E/\lambda$  vs  $\ln E$



$$E/\lambda = E_p^2 [\beta \ln(\gamma E) - C/E + D/E^2] \quad (\text{eV/\AA})$$

$\beta, \gamma, C, D$  -> parameters

For high energies: Fano Plots -> straight line

$$E/\lambda = E_p^2 [\beta \ln(\gamma E) - C/E + D/E^2] \approx E_p^2 \beta \ln(\gamma E)$$

13

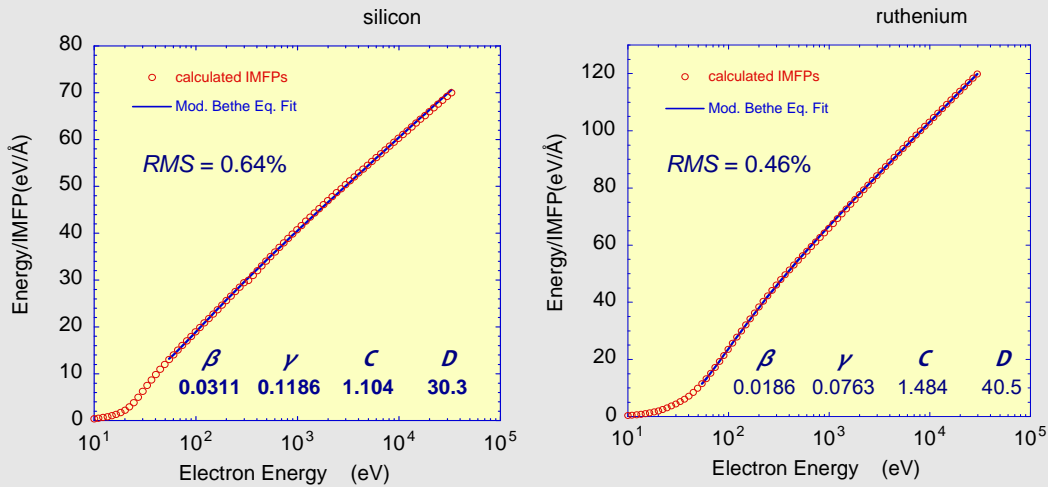
In the analysis of energy dependence of IMFPs, it is convenient to use Fano plots.

Fano plot is expressed as ... the energy over lambda versus log E.

Using Modified Bethe equation, Fano plots can be described by this equation. This has 4 parameters.

## Fano plots for Si and Ru

$$E/\lambda = E_p^2 \left[ \beta \ln(\gamma E) - C/E + D/E^2 \right]$$

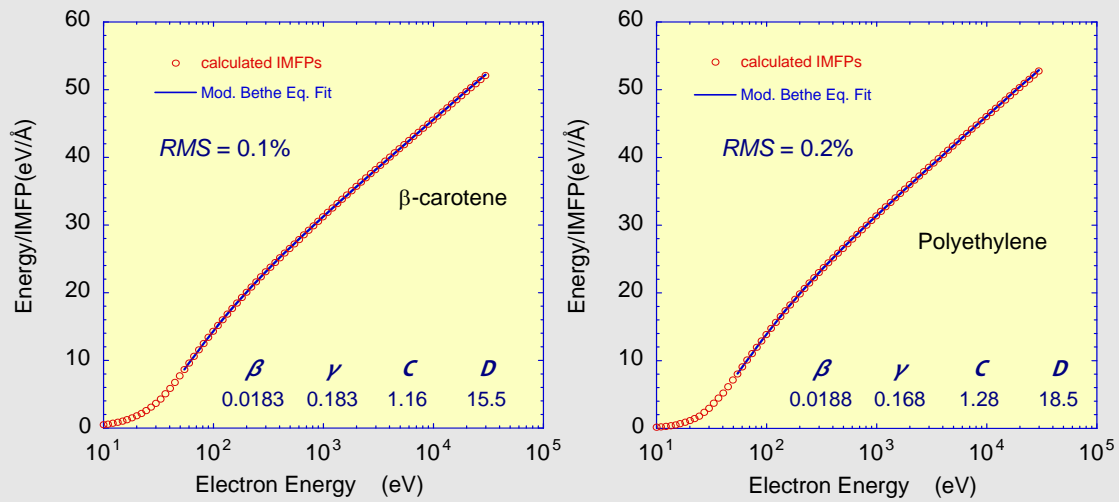


14

These figures show the Fano Plots for Si and Ru and results of curve fits with M. Bethe equation,

The open circles show the calculated IMFPs from optical data. The solid line is the curve fit with Modified. Bethe equation. The curve fits gave excellent results on Si and Ru.

## Fano plots for $\beta$ -carotene and polyethylene



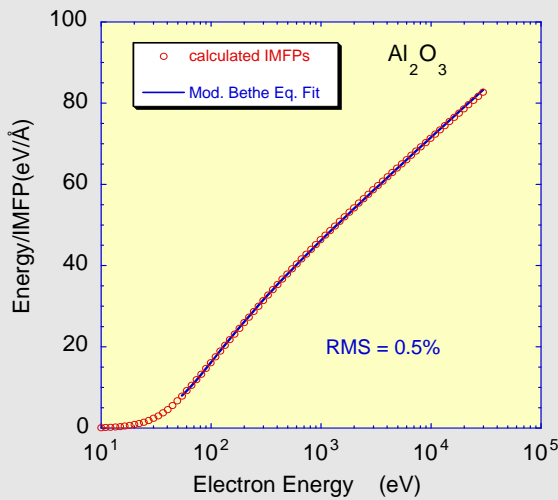
$$E/\lambda = E_p^2 \left[ \beta \ln(\gamma E) - C/E + D/E^2 \right]$$

15

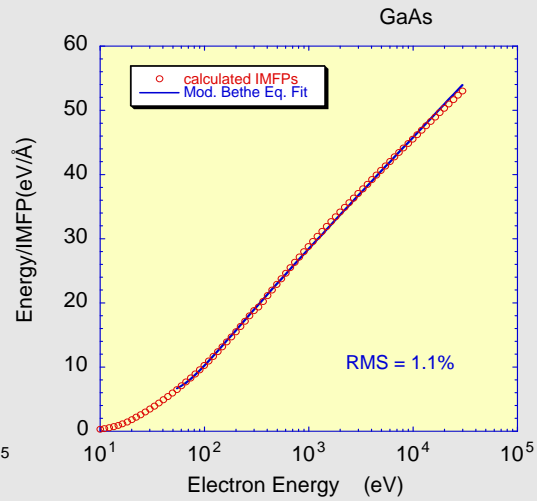
These are the examples of organic compounds. Beta-carotene and polyethylene. The Modified Bethe equation gives also excellent fits for both compounds over 50 to 30 000 eV energy range.

## Fano plots for Al<sub>2</sub>O<sub>3</sub> and GaAs

$$E/\lambda = E_p^2 [\beta \ln(\gamma E) - C/E + D/E^2]$$



$\beta$	$\gamma$	$C$	$D$
0.0146	0.0815	1.16	31.1



$\beta$	$\gamma$	$C$	$D$
0.0306	0.0469	1.05	53.4

16

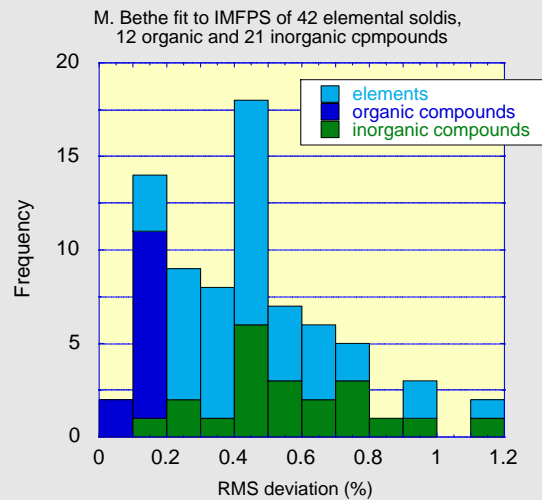
These are the examples of inorganic compounds. Al<sub>2</sub>O<sub>3</sub> and GaAs. For Al<sub>2</sub>O<sub>3</sub>, M. Bethe fit show a good agreement for with energy range. For GaAs, the agreement is not good at higher energy region. This compounds is the worst case in 75 materials in this study. Fortunately, the difference is not so large,

## Results of Modified Bethe equation fits to calculated IMFPs over the 50 eV to 30,000 eV range

- Average RMS deviation

- 42 elemental solids : 0.47 %
- 12 organic compounds : 0.12 %
- 21 inorganic compounds : 0.56 %

Modified Bethe equation could be used to fit IMFPs over the 50 eV to 30,000 eV energy range with low RMS deviations (less than 1.1%)  
GaAs and Co were the worst case!



17

I will show the results of modified Bethe equation fits to calculated IMFPs over the 50 to 30, 000 eV energy range.

This show the histograms of the curve fit results using % of rms errors. The average of rms error of elements is 0.5%,.....

These values are very nice results.

Then, Modified Bethe equation could be used to fit IMFPs over the 50 to 30,000 eV with low rms deviations.

## TPP-2M equation for IMFPs

$$\lambda = \frac{E}{E_p^2 [\beta \ln(\gamma E) - CE^{-1} + DE^{-2}]}$$

$$\beta = -0.10 + 0.944 (E_p^2 + E_g^2)^{-0.5} + 0.069 \rho^{0.1}$$

$$\gamma = 0.191 \rho^{-0.5}$$

$$C = 1.97 - 0.91U$$

$$D = 53.4 - 20.8U$$

$$U = \frac{N_v \rho}{M} = \frac{E_p^2}{829.4}$$

$M$ : atomic or molecular weight

$\rho$ : density

$N_v$ : number of valence electrons

$E_g$ : band-gap energy

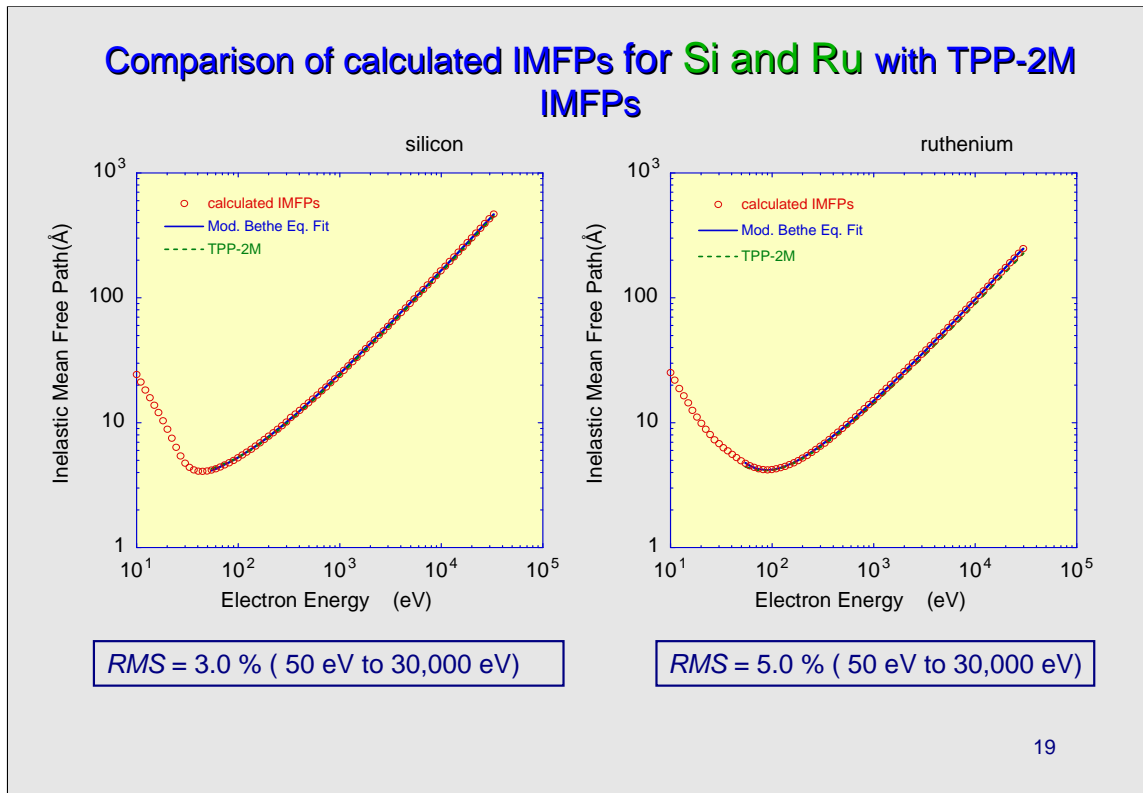
- original energy range: 50 eV to 2000 eV (now extended to 30 keV)
- based on IMFP data for 27 elemental solids and 14 organic compounds

18

S. Tanuma, C. J. Powell, and D. R. Penn, Surf. Interface Anal. **21**, 165 (1994).

Then, We have developed the general formula TPP-2M empirically from the curve fit results with M. Bethe equation. Using this equation, we can estimate the IMFPs in the 50 – 30000eV at any material. IMFP can be calculated with these 4 physical parameters.

From now, we will compare the present calculated IMFPs with those of TPP-2M equation.

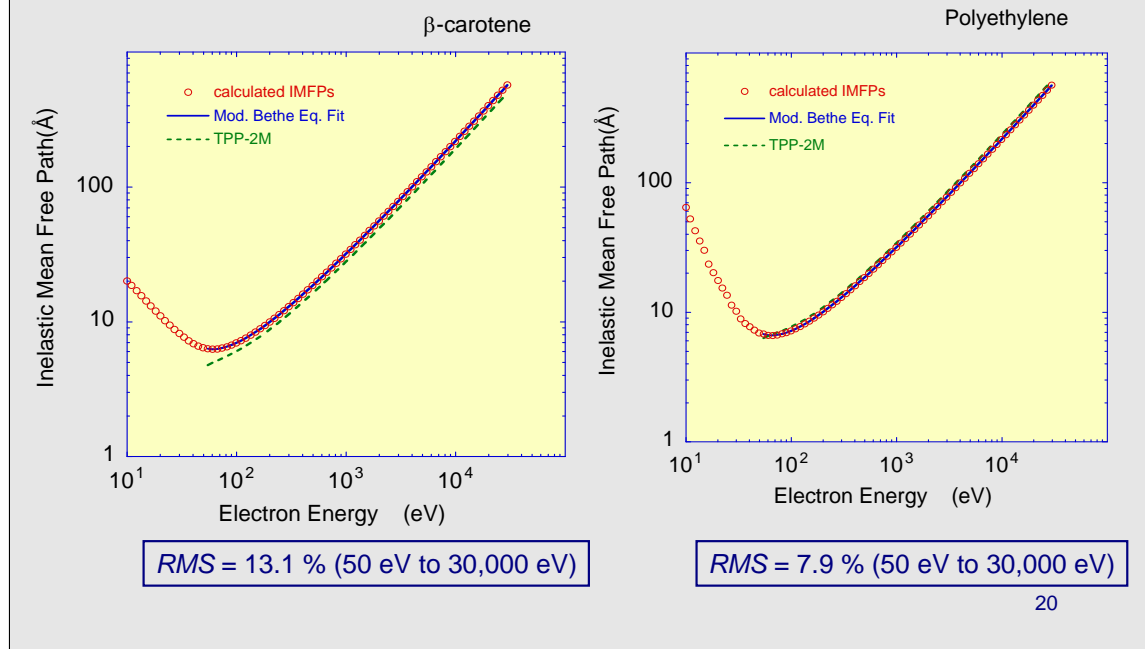


These figures shows the comparison of calculated IMFPs from optical ELF and those of TPP-2M. This is silicon. This is ruthenium. Red circles show the calculated IMFPs, Blue solid line is the results of the curve fit with M. Bethe equation.

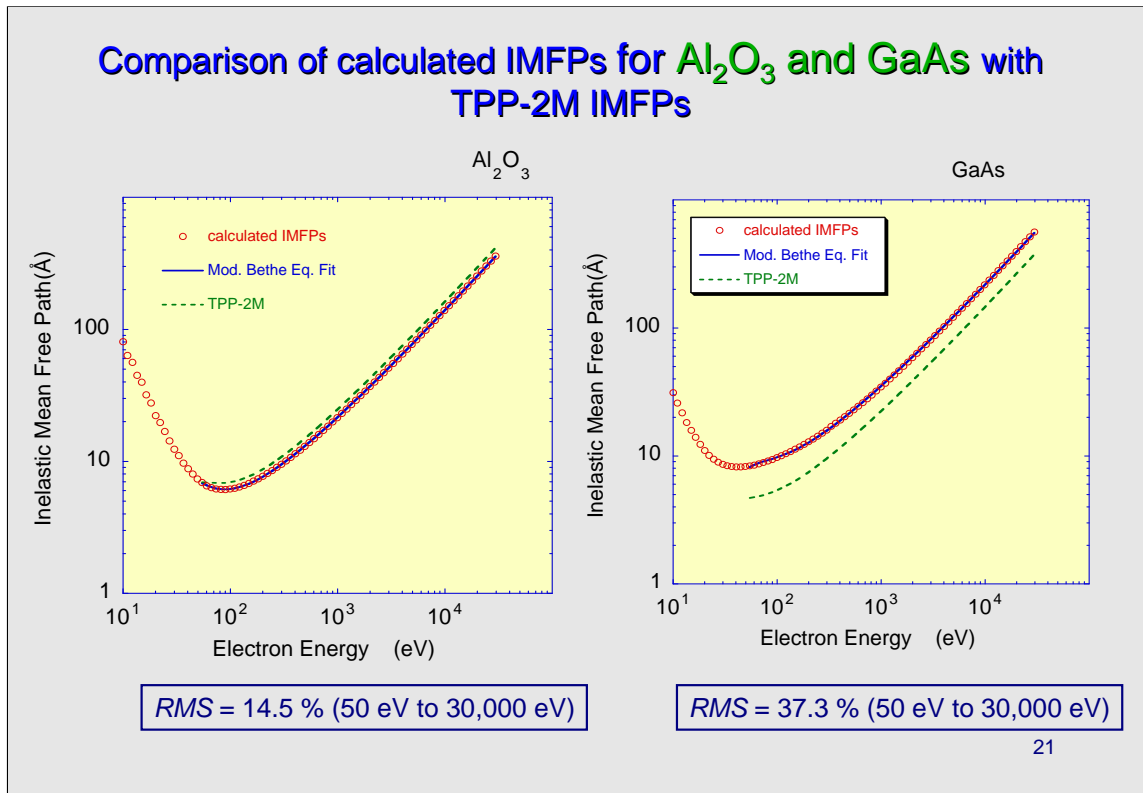
Green doted line show the IMFPs of TPP-2M.

For both elements, the TPP-2M IMFP values are in good agreement with those of calculated IMFPs over 50 - 3000 eV energy range, The rms deviations are 3.0 % and 5 %.

## Comparison of calculated IMFPs for $\beta$ -carotene and polyethylene with TPP-2M IMFPs

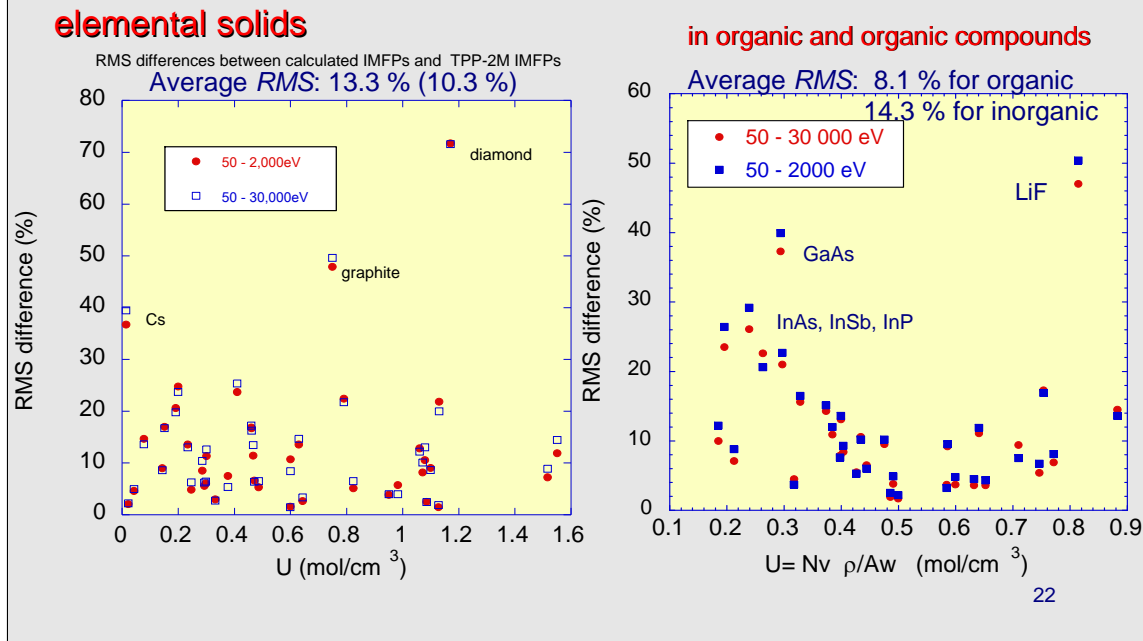


These are the results of organic compounds. For beta carotene, TPP-2M shows the lower IMFP values over 50 - 30 000 eV compared to optical IMFPs. For polyethylene, the TPP-2M IMFPs are in good agreement with calculated IMFPs. Its rms difference is 8%.



These are the results of inorganic compounds. For  $\text{Al}_2\text{O}_3$ , the IMFP values calculated from TPP-2M are larger than the optical IMFPs over 50 to 30,000 eV. On the other hand TPP-2M gives lower values for GaAs like this. The difference is rather large.

RMS differences between calculated IMFPs (from optical energy-loss functions) and TPP-2M IMFPs over the 50 eV to 30,000 eV energy range:



This shows the RMS differences between calculated IMFPs and TPP-2M IMFPs for elemental solids as a function of valence electron density. The average rms is 13 % for 42 elemental solids over 50 to 30,000 eV energy range.

This figure show the rms differences as function of the valence electron density  $U$  for element. Cs, graphite diamond show the large difference. Except these elements, the rms decreases to 10 %.

This is the results for compounds.

The average rms is 8 % organic compounds and 14 % for inorganic compounds.

However, Lithium fluoride and gallium arsenide gave large rms differences. These are mainly

## Summary of IMFP calculations

- We have calculated IMFPs for 50 eV to 30,000 eV electrons in 42 elemental solids, 12 organic compounds, and 21 inorganic compounds using their energy-loss functions and the Penn algorithm. The IMFPs were calculated at equal energy intervals on a logarithmic scale corresponding to increments of 10 %.
- These IMFPs could be fitted to the modified Bethe equation for inelastic scattering of electrons in matter for energies from 50 eV to 30,000 eV. The average RMS deviations in these fits were 0.1 % (organic) and 0.5 % (elements and inorganic compounds).

23

This RMS values are almost the same as those found in our fits of IMFPs calculated previously for the 50 - 2000 eV energy range.

## Summary (continued)

- The optical IMFPs were also compared with IMFPs from the TPP-2M equation; the average RMS deviations were 13 % (elements), 8 % (organic compounds) and 14 % (inorganic compounds) for energies from 50 eV to 30,000 eV.
- Relatively large RMS deviations were found for diamond, graphite, and cesium in the elements group. If these elements were excluded, the average RMS deviation was 10.3 %. Large deviations were also found for GaAs and LiF.
- We conclude that the TPP-2M equation is useful for IMFP estimation in other materials for energies up to 30,000 eV with an average uncertainty of about 11 %.

S. Tanuma, C. J. Powell, and D. R. Penn, Surf. Interface Anal. **37**, 1 (2005).

24

### 3. Experimental Determination of Electron Inelastic Mean Free Paths by Elastic-Peak Electron Spectroscopy (EPES)

- assess the reliability of IMFPs calculated from energy-loss functions with the Penn algorithm (optical IMFPs) and from the TPP-2M equation.
- determine IMFPs for Ag, Au, Cr, Cu, Fe, Ga, C (graphite), Mo, Pt, Si, Ta, W, and Zn over the 50 eV to 5,000 eV energy range from backscattered elastic-peak intensities (EPIs) using a Ni reference material.

C. J. Powell and A. Jablonski, J. Phys. Chem. Ref. Data **28**, 19 (1999).

S. Tanuma, T. Shiratori, T. Kimura, K. Goto, S. Ichimura, and C. J. Powell, Surf. Interface Anal. **37**, 833 (2005). 25

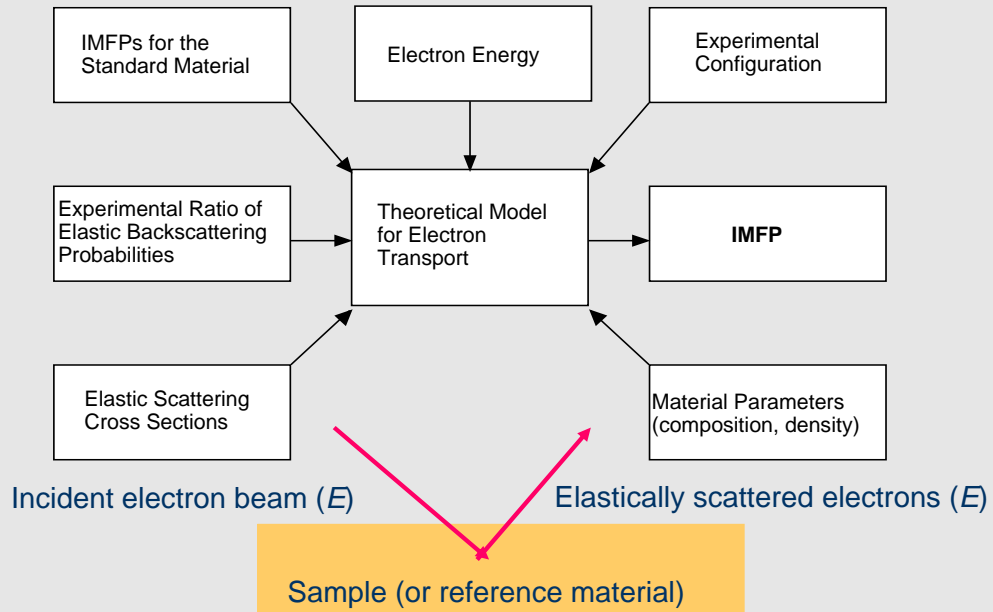
From now, I will talk about the experimental determination of...

It is very important to know....

We have determine

We will compare the resulting experimental IMFPs with the

## Elastic-peak electron spectroscopy (EPES)



## Measurements of EPIs by absolute CMA

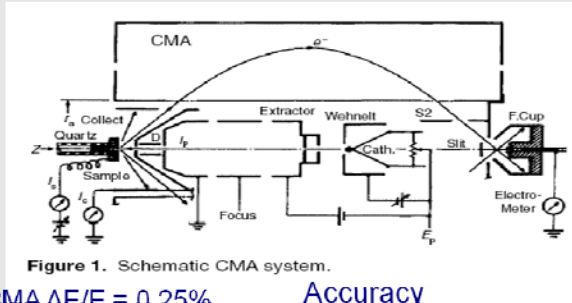
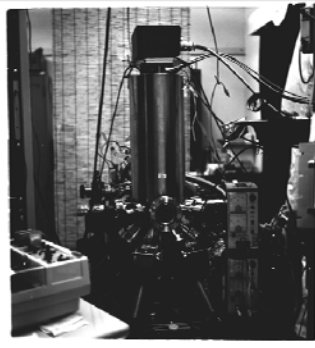


Figure 1. Schematic CMA system.

$CMA \Delta E/E = 0.25\%$

Accuracy

$\pm 0.01\%$  (primary beam energy)

$\pm 0.5\%$  (Auger spectra)

Measurement of Elastic Peak Intensity

Energy range : 1 eV to 5,000 eV

(50 eV to 5,000 eV)

Instrument: Absolute Auger Spectrometer

-detection angle ( $42.3 \pm 6^\circ$ )

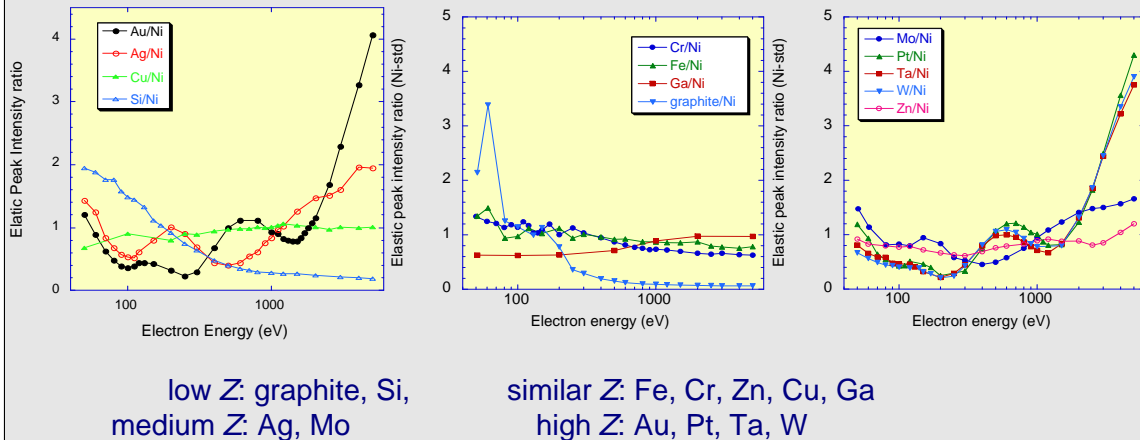
Primary beam:  $1 \mu A$

Detector: Faraday cup

27

This slide shows the instrument used for the measurement of elastic peak intensities. This system was made by Professor Goto. This system have a CMA and the detector is Faraday cup to measure the electron current directly. The measurements of EPIs were done in 1 to 5000 eV energy range.

## Measured elastic-peak intensity ratios (with respect to Ni) as a function of electron energy



28

This viewgraph show the measured elastic peak intensity ratios as functions of electron energy for 13 elemental solids using Ni reference.

classify things *into* three types 物を4種に分類する

このあとは論文から引用．パターンはにている．原子番号に良く依存

Low atomic number : graphite, silicon

Middle atomic number: Fe, Cr, Zn, Cu, Ga

## Calculation of Elastic-Peak Intensities from Monte Carlo Simulations

Instrumental function

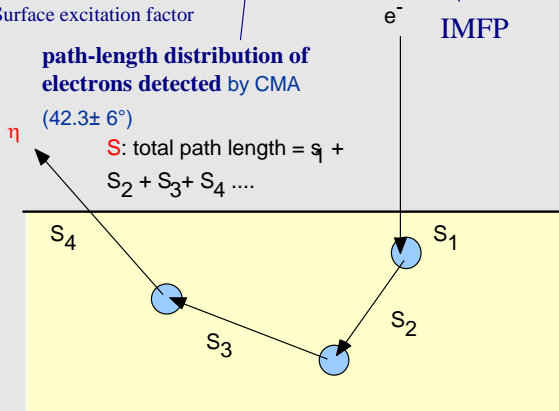
$$I = G_t \times f_s \times \int_0^\infty \left( \frac{d\eta}{dS} \right) / N_0 \exp\left(-\frac{S}{\lambda}\right) dS$$

Surface excitation factor

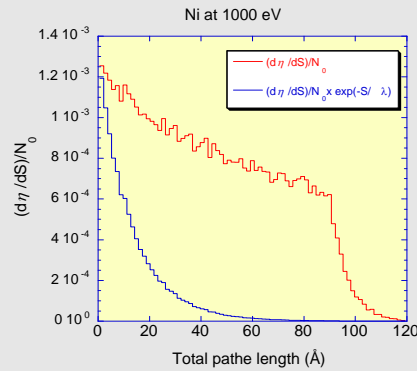
path-length distribution of electrons detected by CMA

(42.3 ± 6°)

S: total path length = s<sub>1</sub> + s<sub>2</sub> + s<sub>3</sub> + s<sub>4</sub> ...



IMFP



:Elastic-scattering cross sections from the Thomas-Fermi-Dirac potential  
:Pseudo random number generator Mersenne Twister

29

This one show the calculation of ..., From Monte Carlo method, we can calculate the peak intensity from this equation.

The  $G_t$  is a instrumental factor; mainly due to the transmission efficiency of CMA mesh.  $f_s$  is surface-excitation factor....

$S$  means the total path length.

This graph is an example of the histograms of path length distribution.

In MC calculation, pseudo random number generator is very important. We use Mersenne twister which was developed by Matsumoto.

It is proved that the period is  $2^{19937}-1$ , and the 623-dimensional equidistribution property is assured

## Calculation of Elastic-Peak Intensity Ratio to Ni Reference

Determination of IMFPs from EPIs using Ni standard

; remove  $G_t$

$$f_s^x / f_s^{Ni} = 1 \quad - \text{Assume initially that surface-excitation effects are negligible}$$

$$\left( \frac{I^x}{I^{Ni}} \right)_{cal} = \frac{\int_0^{\infty} (d\eta/dS)^x / N_0^x \exp(-S/\lambda_x) dS}{\int_0^{\infty} (d\eta/dS)^{Ni} / N_0^{Ni} \exp(-S/\lambda_{Ni}) dS}$$

Determination of IMFPs using Ni standard

Then,

$$\left[ \left( \frac{I^x}{I^{Ni}} \right)_{measured} - \left( \frac{I^x}{I^{Ni}} \right)_{cal} \right]^2 \rightarrow min$$

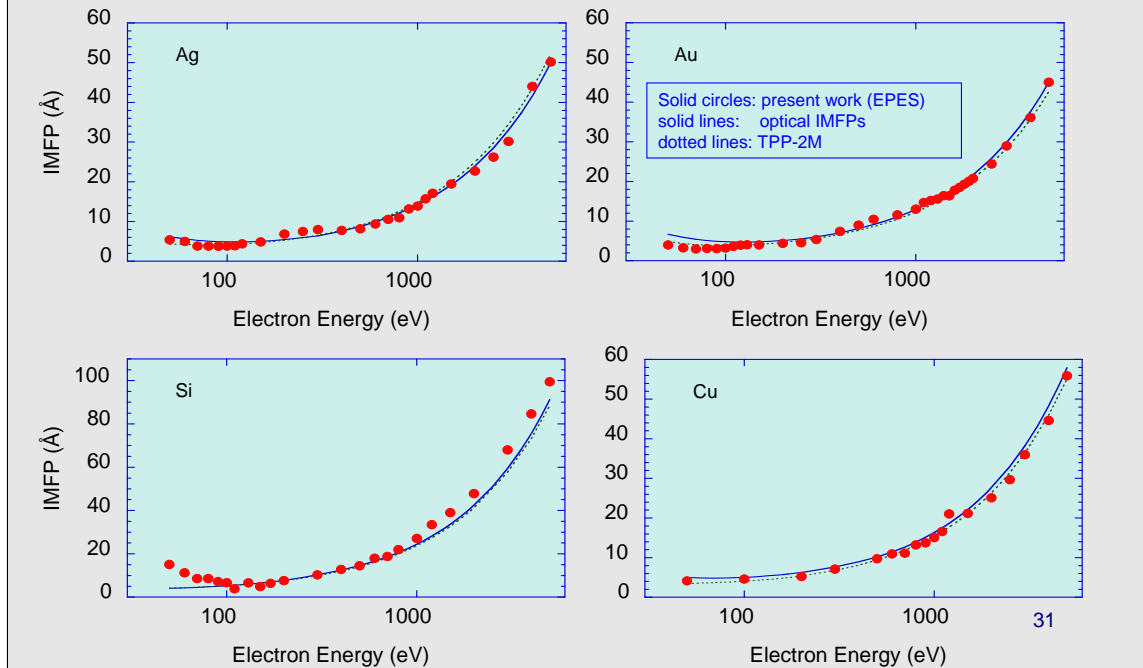
Solve above equation for parameter  $\lambda_x$  (IMFP) for the target material using optical IMFP for  $\lambda_{Ni}$  (with solver in Excel)

30

Using path length distributions of Ni-reference and the target material, the peak intensity ratio can be described by this equation.

Then, optimizing this condition, we can get lambda x for target material. This calculations can be done easily with solver command in excel.

## IMFPs determined from EPI ratios for Au, Ag, Si, and Cu



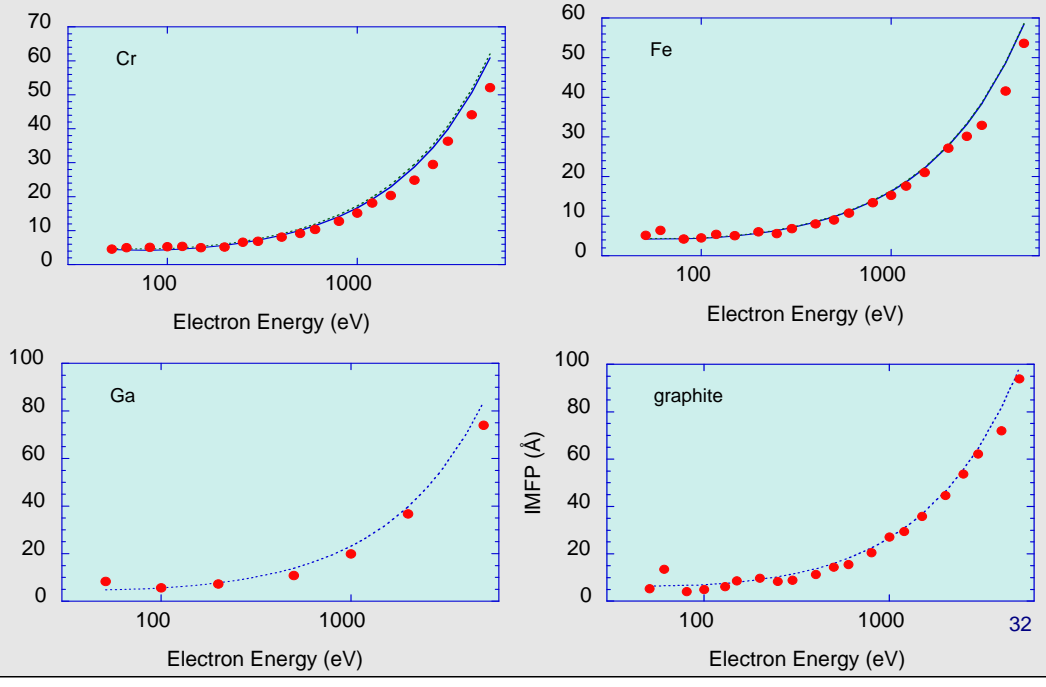
This viewgraph shows the determined IMFPs of Ag, Au, Si and Cu from their elastic peak in the 50 to 5000 eV,.

The solid circles....

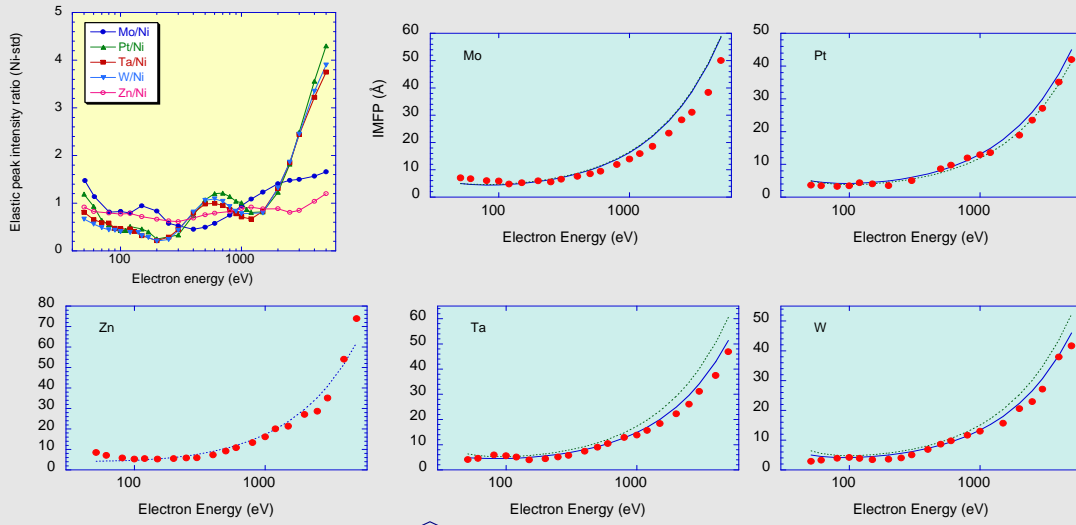
In Au, Ag, Cu, the present IMFPs from EPES are in excellent agreement with theoretical values over 200 eV region like this.

However, in Si the EPES-IMFPs coincide well with optical and TPP-2M IMFPs in the 100 to 1000 eV. Over 1000 and under 100 eV region, the determined IMFPs are larger than the theoretical values.

# IMFPs determined from EPI ratios for Cr, Fe, Ga, and Graphite



# IMFPs determined from EPI ratios for Mo, Pt, Zn, Ta, and W

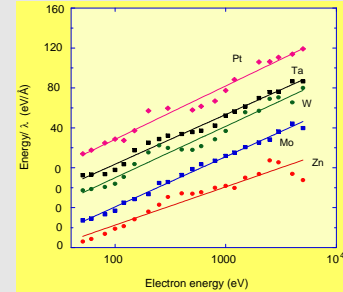
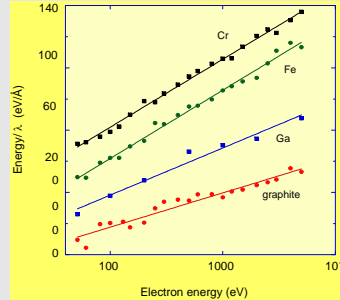
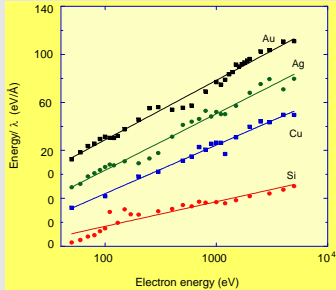


Solid circles: present work (EPES) , solid lines: optical IMFPs, dotted lines: TPP-2M

# Analysis of IMFPs with Fano Plot

- We have analyzed experimentally determined IMFPs using Fano Plots which were constructed by plotting values of  $E/\lambda$  versus  $\ln E$ .

$$E/\lambda = b + a \ln(E)$$



solid symbols : experimentally determined IMFPs  
 solid lines: fit to the energy/IMFP values with the Bethe equation

$$E/\lambda = E_p^2 \beta \ln(\gamma E)$$

← Simple Bethe equation

34

Since the data points lie sufficiently close to straight lines, Fano plot can be fit by simple Bethe equation.

Then the values of the parameters beta and gamma were found from a linear least-squares analysis.

RMS difference of IMFPs determined by EPES from optical IMFPs (Penn algorithm) and IMFPs from the TPP-2M equation

Element	RMS difference (%)		
	Optical IMFP		TPP-2M IMFP $E_{\min} = 100 \text{ eV}$
	$E_{\min} = 100 \text{ eV}$	$E_{\min} = 200 \text{ eV}$	
Graphite	27.0	27.4	8.9
Si	8.9	8.4	11.2
Cr	9.1	9.9	12.7
Fe	7.0	7.6	7.7
Cu	10.7	9.1	1.9
Zn	-	-	5.7
Ga	-	-	12.1
Mo	15.9	17.2	16.9
Ag	3.7	1.7	4.4
Ta	8.7	9.0	26.4
W	11.3	9.8	25.7
Pt	9.1	8.0	2.4
Au	10.0	4.2	3.6
Average RMS difference:	11.0	10.2	10.7

Average RMS (100 eV to 5000 eV):  
11.0 % (optical)  
10.7 % (TPP-2M)

<sup>a</sup> Optical IMFPs are not available for Zn and Ga.

35

finally I will show you the results of IMFP comparison.

This is the results of the comparison with optical IMFPs and, this is the results with TPP-2M.

The average rms is ..

# Summary

- We have performed experimental determinations of IMFPs for 13 elemental solids over the 50 eV to 5000 eV energy range from backscattered elastic-peak intensities using a Ni reference together with Monte Carlo simulations.
- These IMFPs determined could be fitted with the simple Bethe formula over the 100 eV to 5000 eV energy range using Fano plots (average RMS deviation: 9 %)
- The IMFPs of Ag, Au, Cr, Cu, Fe, Pt, Si, Ta, and W were in excellent agreement (RMS deviations less than 11%) with those calculated from the Penn algorithm (optical IMFPs) over the 100 eV to 5000 eV energy range.

- We conclude that the accuracy of IMFPs for elemental solids calculated from measured energy-loss functions is about 10 % over the 100 eV to 5000 eV energy range.

## 4. IMFP Applications

- Quantitative XPS [1]
- Other important parameters [2]:
  - Effective attenuation lengths (EALs)
  - Mean escape depths (MEDs)
  - Information depths (IDs)
- Modeling XPS for Thin-Film Structures [3]

1. C. J. Powell and A. Jablonski, *J. Electron Spectrosc. Relat. Phenom.* (in press).
2. C. J. Powell and A. Jablonski, *Nucl. Instr. Methods Phys. Res. A* **601**, 54 (2009).
3. W. S. M. Werner, W. Smekal, and C. J. Powell, *Surf. Interface Anal.* **37**, 1059 (2005).

## Effective Attenuation Lengths

The effective attenuation length (EAL) is the parameter to be used in an equation in place of the IMFP to account for the effects of elastic scattering.

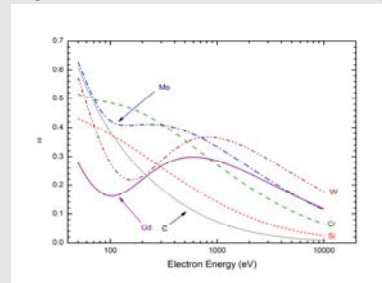
Jablonski and Powell [1] proposed a simple empirical formula for the average **EAL for film-thickness measurements**,  $L$ , for emission angles between  $0^\circ$  and  $50^\circ$ :

$$L = \lambda_{in} (1 - 0.735 \omega)$$

$$\omega = \frac{\lambda_{in}}{\lambda_{in} + \lambda_{tr}}$$

where  $\lambda_{in}$  is the IMFP and  $\lambda_{tr}$  is the transport mean free path (TMFP) which is derived from the differential cross section for elastic scattering. This formula was developed for electron energies between 100 eV and 2 keV, but should be valid for higher energies.

The plot shows  $\omega$  as a function of electron energy for six illustrative elemental solids [2].



1. A. Jablonski and C. J. Powell, J. Vac. Sci. Technol. A **27**, 253 (2009).
2. C. J. Powell and A. Jablonski, J. Electron Spectrosc. Relat. Phenom. (in press).

## Mean Escape Depths

The mean escape depth (MED) is the average depth normal to the surface from which the detected electrons escape.

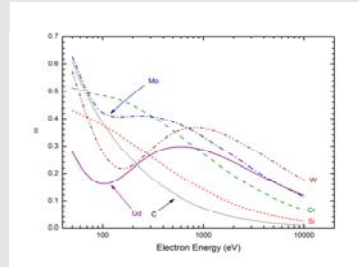
In the absence of elastic scattering, the MED,  $D$ , is  $D = \lambda_{in} \cos \alpha$  where  $\alpha$  is the electron emission angle (with respect to the surface normal).

When elastic scattering is considered, an empirical formula for  $D$  proposed by Jablonski and Powell [1] can be used for emission angles between  $0^\circ$  and  $50^\circ$ :

$$D = \lambda_{in} \cos \alpha (1 - 0.736\omega)$$

This formula was developed for electron energies between 100 eV and 2 keV, but should be valid for higher energies.

$$\omega = \frac{\lambda_{in}}{\lambda_{in} + \lambda_{tr}}$$



1. A. Jablonski and C. J. Powell, J. Vac. Sci. Technol. A **27**, 253 (2009).

## Information Depths

The information depth (ID) is the depth normal to the surface from which useful signal information is obtained.

In the absence of elastic scattering, the ID,  $S$ , is where  $P$  is a specified percentage of the detected signal.

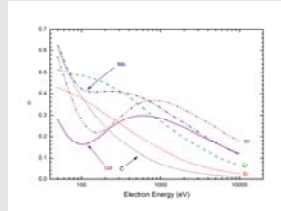
$$S = \lambda_{in} \cos \alpha \ln \left[ \frac{1}{1 - (P/100)} \right]$$

When elastic scattering is considered, an empirical formula for  $S$  proposed by Jablonski and Powell [1] can be used for emission angles between  $0^\circ$  and  $50^\circ$ :

$$S = \lambda_{in} \cos \alpha (1 - 0.787\omega) \ln \left[ \frac{1}{1 - (P/100)} \right]$$

This formula was developed for electron energies between 100 eV and 2 keV, but should be valid for higher energies.

$$\omega = \frac{\lambda_{in}}{\lambda_{in} + \lambda_{tr}}$$

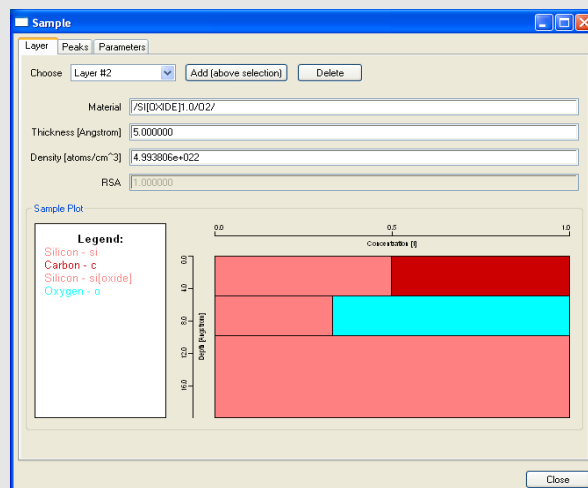


1. A. Jablonski and C. J. Powell, J. Vac. Sci. Technol. A **27**, 253 (2009).

## Modeling XPS for Thin-Film Structures

The NIST Database for Simulation of Electron Spectra for Surface Analysis (SESSA) [1,2] provides data for quantitative XPS for X-ray energies up to 20 keV. SESSA can also perform efficient Monte Carlo simulations of XPS spectra for multi-layered thin-film samples.

Version 1.2 of SESSA (expected to be released in fall, 2009) will include the capability to perform XPS simulations with varying amounts of X-ray polarization (both linear and circular). This capability will make SESSA useful for XPS applications with synchrotron radiation.

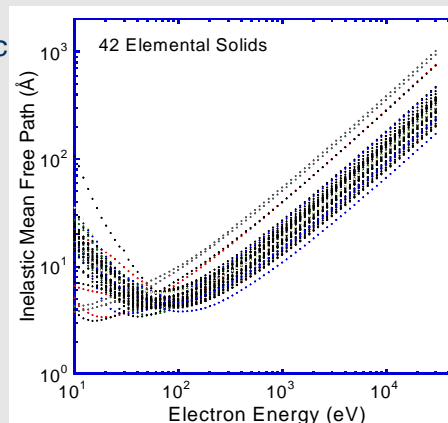


1. <http://www.nist.gov/srd/nist100.htm>.

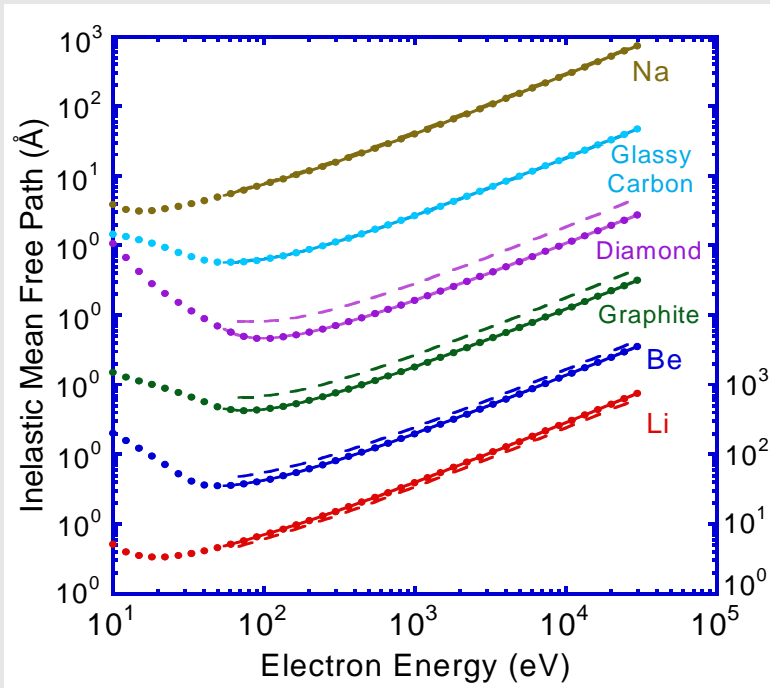
2. W. Smekal, W. S. M. Werner, and C. J. Powell, Surf. Interface Anal. **37**, 1059 (2005).

## 5. Summary

1. IMFPs have been calculated for 42 elemental solids, 12 organic compounds, and 21 inorganic from experimental optical data for electron energies from 50 eV to 30 keV.
2. The modified Bethe equation fits the optical IMFPs well over the entire energy range.
3. The TPP-2M equation provides reasonable estimates of IMFPs over the entire energy range (although there were large deviations for graphite, diamond, Cs, GaAs, and LiF).
4. IMFPs from elastic-peak electron spectroscopy experiments generally agree well with the optical IMFPs.
5. Simple analytical formulae have been developed to provide useful estimates of effective attenuation lengths (for film-thickness measurements), mean escape depths, and information depths (for estimates of surface sensitivity). These formulae enable convenient corrections for elastic-scattering effects (for  $\alpha \leq 50^\circ$ ).
6. The NIST SESSA database provides physical data (including IMFPs from the TPP-2M equation) for energies up to 20 keV. A planned enhancement will enable simulations of XPS spectra with polarized X-rays.



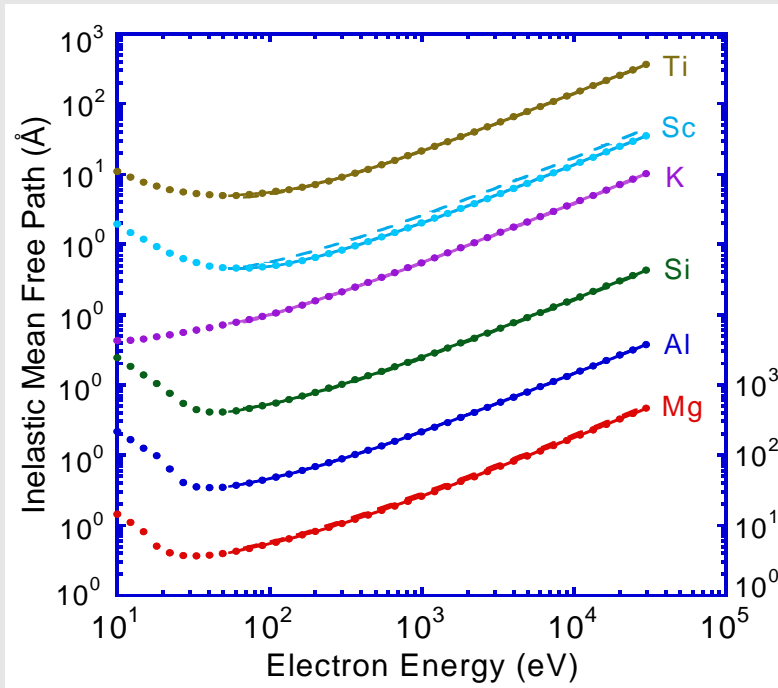
Optical IMFPs (points) for Li, Be, graphite, diamond, glassy C, and Na



Solid lines show fits with the modified Bethe equation

Dashed lines show IMFPs from the TPP-2M equation

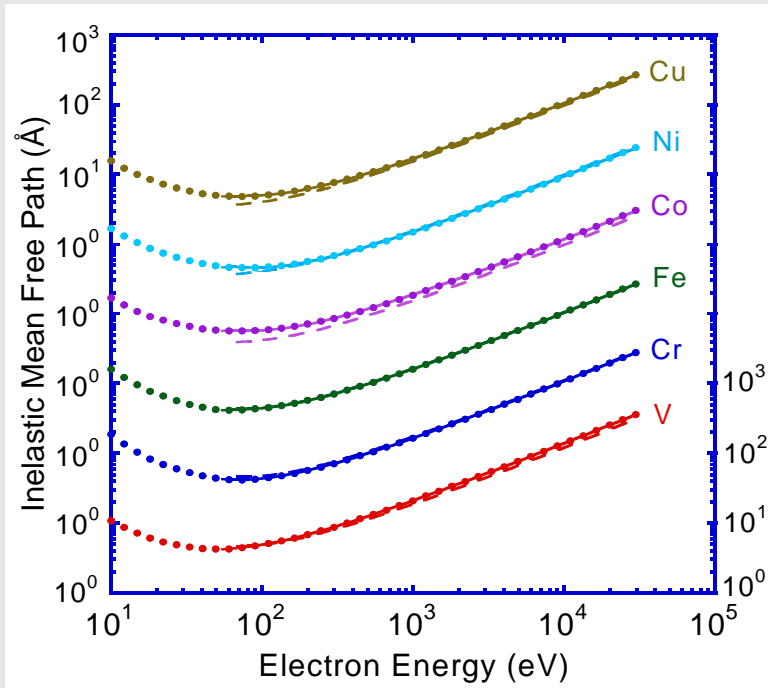
Optical IMFPs (points) for Mg, Al, Si, K, Sc, and Ti



Solid lines show fits with the modified Bethe equation

Dashed lines show IMFPs from the TPP-2M equation

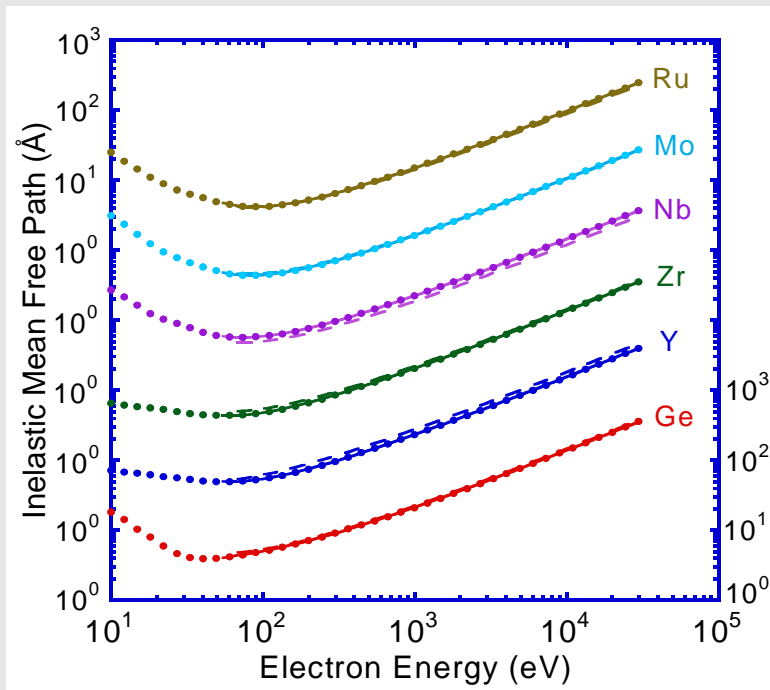
Optical IMFPs (points) for V, Cr, Fe, Co, Ni, and Cu



Solid lines show fits with the modified Bethe equation

Dashed lines show IMFPs from the TPP-2M equation

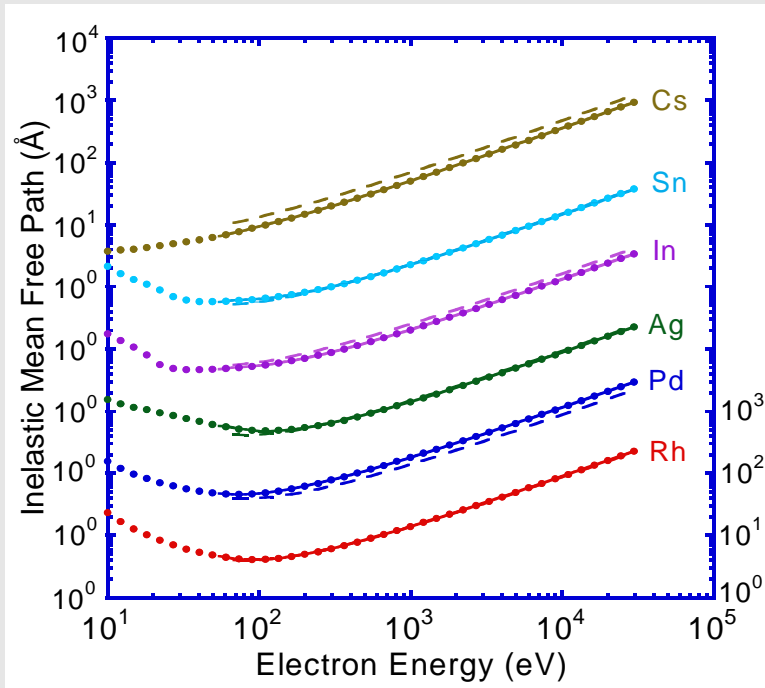
Optical IMFPs (points) for Ge, Y, Zr, Nb, Mo, and Ru



Solid lines show fits with the modified Bethe equation

Dashed lines show IMFPs from the TPP-2M equation

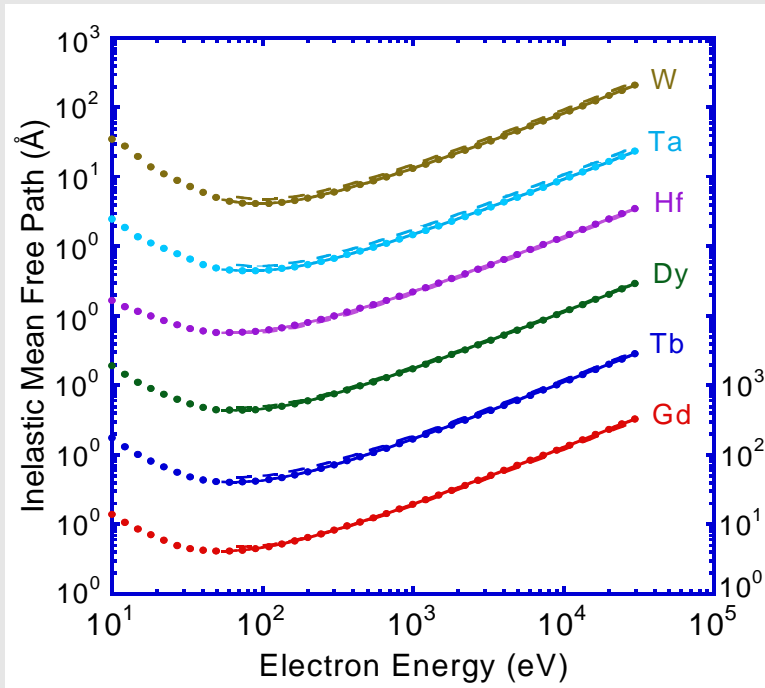
Optical IMFPs (points) for Rh, Pd, Ag, In, Sn, and Cs



Solid lines show fits with the modified Bethe equation

Dashed lines show IMFPs from the TPP-2M equation

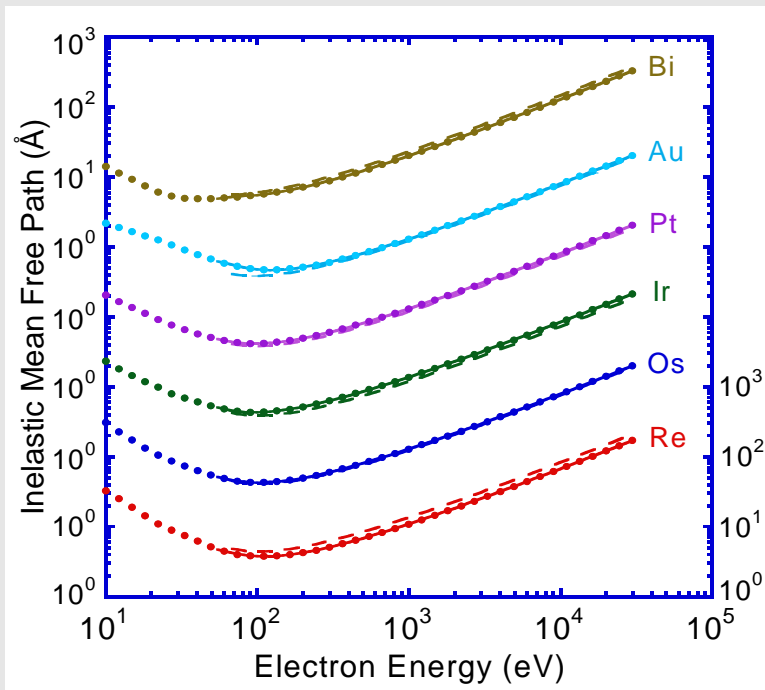
Optical IMFPs (points) for Gd, Tb, Dy, Hf, Ta, and W



Solid lines show fits with the modified Bethe equation

Dashed lines show IMFPs from the TPP-2M equation

Optical IMFPs (points) for Re, Os, Ir, Pt, Au, and Bi



Solid lines show fits with the modified Bethe equation

Dashed lines show IMFPs from the TPP-2M equation